J Solid State Electrochem (2011) 15:765–771
DOI 10.1007/s10008-010-1155-0

ORIGINAL PAPER

Molding versus dispersion: effect of the preparation procedure on the capacitive and cycle life of carbon nanotubes aerogel composites

Tarik Bordjiba · Mohamed Mohamedi

Received: 28 April 2010 / Revised: 20 July 2010 / Accepted: 23 July 2010 / Published online: 1 August 2010

Abstract Binderless carbon nanotubes aerogel (CNAG) composites represent a new class of high-performing electrodes for energy storage applications such as electrochemical double layer capacitors. The composites developed here differ significantly from these previously prepared with dispersion processes. The CNAG material was prepared by a molding procedure that is the synthesis by a chemical vapor deposition method to grow carbon nanotubes directly onto a microfibrous carbon paper substrate. Then the carbon aerogel is synthesized on the carbon nanotubes. The key feature of the method is eliminating the need of controlling the carbon nanotube concentration, which permits optimized dispersion processes to reinforce the aerogel's networks. The CNAG electrode delivered very high specific capacitances of 524 F g^{-1} in KOH electrolyte and 280 F g^{-1} in H_2SO_4 electrolyte. Furthermore, this better integration of carbon nanotubes in the matrix of carbon aerogel improved its resistance to the attack by the electrolyte and conferred an excellent cycle life over 5,000 cycles of charge–discharge in both electrolytes.

T. Bordjiba (✉) · M. Mohamedi
Énergie, Matériaux et Télécommunications,
Institut National de Recherche Scientifique, INRS,
1650 Blvd. Lionel Boulet,
Varennes, QC, Canada J3X 1S2
e-mail: bordjiba_tarik@yahoo.ca

Present Address:
T. Bordjiba
Département de Chimie, Université du Québec à Montréal,
Case Postale 8888, succursale Centre-Ville,
Montréal, QC H3C 3P8, Canada

Introduction

Recent trends in electrochemical capacitor technology involve the development of high surface area activated carbon electrodes to optimize the performance in terms of capacitance and overall conductivity [1, 2].

Attention has been focused on nanostructured carbons such as aerogels [3–11]. Carbon aerogels (CAGs) are novel ultralight materials with many interesting properties such as low mass densities, continuous porosities, high surface areas, and high electrical conductivity. These properties are derived from the aerogel microstructure, which is a network of interconnected primary particles with characteristic diameters between 3 and 25 nm (Scheme 1a). However, aerogels are constituted of agglomerate particles linked by covalent bridges (ladder structure). The contact between these particles and the space due to the pores unfortunately introduce a high internal resistance within the aerogel which can be detrimental for electricity generation applications.

To overcome this issue, the approach is to introduce carbon nanotubes (CNTs) into the porous matrices of the aerogel itself. Because of their high electrical conductivity, CNTs are expected to work as nanocollecteurs (nanopathways for charges) and thus improve the intrinsic conductivity of the CAGs and their mechanical tenure as well (Scheme 1b).

Making such nanostructured composites freestanding (100% free binders) and built with electrically conductive substrates would make them further interesting in electrochemical power sources applications. Indeed, binderless nanostructured electrodes will not only improve the performance but also alleviate the cost of manufacturing and avoid the complicated interferences of the binders and conductivity enhancers used in practical electrodes. Such

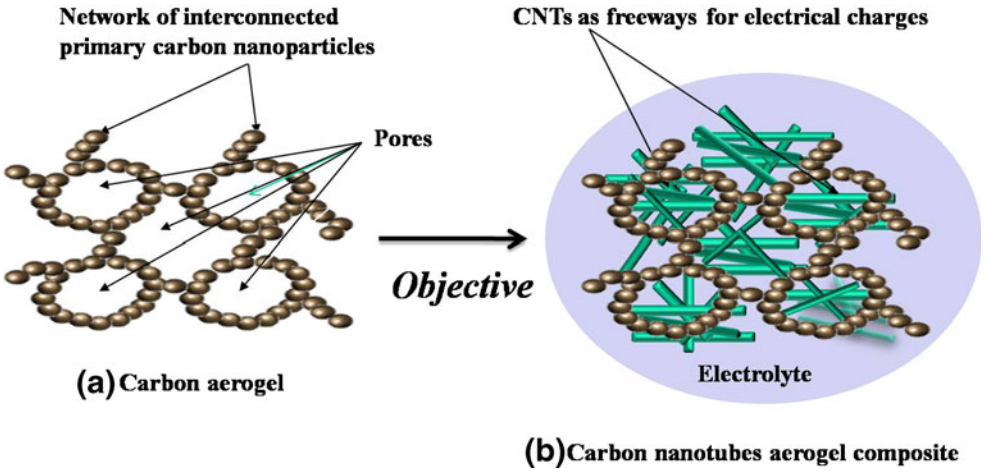

Scheme 1 **a** Representation of the carbon aerogel internal structure and **b** targeted carbon nanotube aerogel composite

structures could thus constitute the next generation electrodes in energy conversion and storage applications.

Our group is being active into the development of such freestanding nanostructures for the specific electrochemical energy storage and conversion applications [12–18].

As to the CAG–CNT nanocomposites, our first strategy was to synthesize binderless composites CAG (0 to 12 wt.% CNTs) from carbonized polyacrylonitrile (PAN) multiwalled carbon nanotube powder (MWNTs) materials processed from their dispersion in dimethylformamide and the whole was deposited by impregnation onto an electrically conductive microfibrous carbon paper (MFCP) [14–16]. The nanocomposites displayed high specific surface area (SSA) ranging between 670 and 710 $m^2\ g^{-1}$. We measured the highest capacitances with an optimum CAG–MWNT composite containing 3 wt.% of MWNTs displaying a specific capacitance of 232 F g^{-1} in H_2SO_4 versus 218 F g^{-1} in KOH. However, stability upon several thousands of charge–discharge cycling was not satisfactory for this material, i.e., in KOH the sample displayed a 21% loss of its initial capacity, whereas in H_2SO_4, the material lost 78% of its initial capacitance [16]. Higher amount of MWNTs diminished the effective portion of the active electrode material resulting in the reduction of the specific capacitance. These results were not expected since higher amounts of CNTs should theoretically lead to higher specific capacitance. It is likely that MWNTs agglomerated instead of being homogeneously spread within the whole CAG's pore network (Scheme 2). Dispersion preparation processes are rather difficult and still present considerable challenges into the adhesion of nanotubes to the material network, particularly. Indeed, the effective utilization of CNTs in composite applications depends strongly on the ability to disperse them individually and uniformly throughout the host matrix without destroying their integrity or reducing their aspect ratio.

To improve dispersion of carbon nanotubes within the aerogel matrix and develop better interfacial coating, we introduced in a recent communication, a molding procedure in which the CNTs are directly grown onto an MFCP substrate. Afterwards, the CAG is synthesized onto the CNTs [17]. The resulting carbon nanotube aerogel (CNAG) composites have exceptionally high specific capacitance of 524 F g^{-1} when used as an electrode in electrochemical double layer capacitors in KOH electrolyte. This capacitance is almost four times greater than that of CAG alone (134 F g^{-1}) and two times greater than the optimum CAG-3%MWNT (218 F g^{-1}) prepared by dispersion process [14]. The key feature of the molding method is eliminating the necessity of controlling the carbon nanotube concentration, which permits optimized dispersion processes to reinforce the aerogel's networks (Scheme 3).

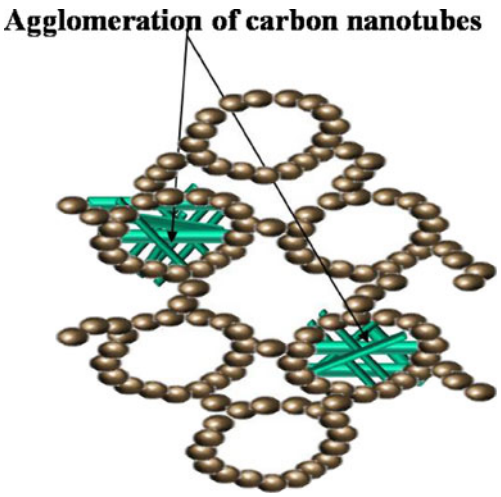

Scheme 2 Carbon nanotube aerogel composite prepared by dispersion procedure

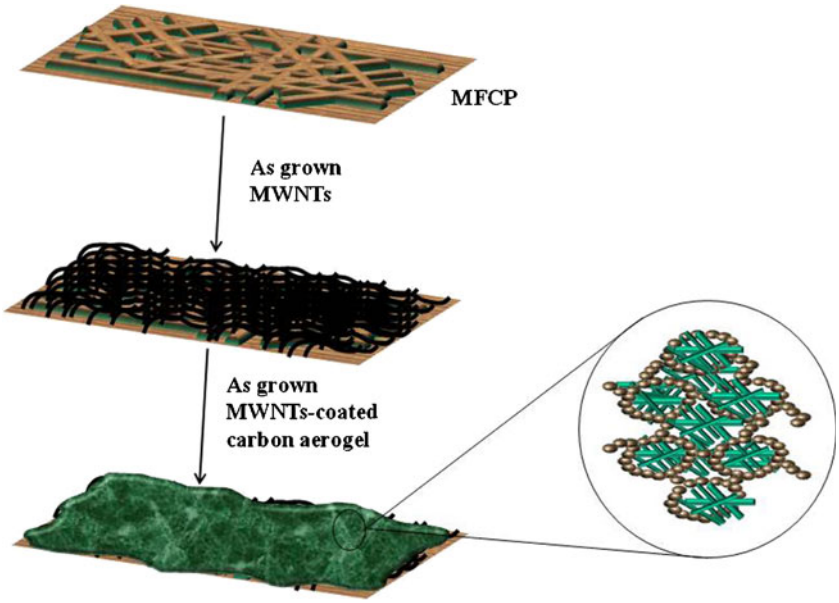

Scheme 3 The concept of the molding process to prepare uniformly distributed carbon nanotubes within the internal network of the carbon aerogel

In this work, we address some unstudied aspects of this new class of CNAG composites and report:

- The full study of their capacitive behaviors in H_2SO_4 electrolyte, an electrolyte that is also of main interest for supercapacitor devices
- Their cycle life upon several thousands of charge–discharge cycles in both KOH and H_2SO_4 electrolytes in order to assess their potentialities as electrodes for electrochemical double layer capacitors
- In order to emphasize the effect of the preparation procedure, results obtained with CNAG composites will always be compared with those obtained with the optimum CAG-3%MWNT composite synthesized with dispersion process.

Experimental

Material synthesis

The synthesis of CAG–MWNT composite by dispersion process is reported in detail elsewhere [14, 16]. The synthesis of the CNAG is also reported elsewhere [17]. Briefly, the incorporation of MWNTs within the ultraporous CAG structure followed three main steps: (1) growth of MWNTs on MFCP by chemical vapor deposition (CVD) method, (2) deposition of aquagel film on MWNTs–MFCP as follows: the MWNTs–MFCP sheets were dipped into a boiling solution of PAN powder (5 g) dissolved in a mixture of dimethylformamide (DMF)/water (84/16 mL). Afterwards, the sheets were dried in air for 10 min and then immersed in acetone overnight. (3) Heat treatment of the aquagel film deposited on MWNTs–MFCP sheets by using pretreatment, carbonization and activation. The pretreatment was performed in air at 215°C for 20 h. This step led to cyclization reactions and to a ladder structure. The carbonization process was performed at 850°C for 8 h in an inert atmosphere (argon) leading to the carbon aerogel. Finally, the activation was done at 850°C under carbon dioxide atmosphere.

Electrochemical studies

Electrochemical measurements were carried out using a three-electrode cell with the reference electrode and counter electrode being an Ag/AgCl, KCl (3 M) and a platinum coil, respectively. The electrolytes were 5 M KOH and 3 M H_2SO_4. The sample electrochemical characteristics were determined by cyclic voltammetry (CV), constant current (CC) charge–discharge techniques. An EG&G galvanostat-potentiostat model 263A was used for CV and CC measurements. The specific capacitance was evaluated from the constant current charge–discharge results using the equation $C = I \times t_d / m\Delta E_{CC}$, where I is the total current, m is the mass of the electrode active material, t_d is the discharge time, ΔE_{CC} is the CC potential drop during constant current discharge.

Results and discussion

Figure 1 shows the typical cyclic voltammograms (CVs) of CNAG electrodes recorded at various potential scan rates ranging from 5 to 100 mV s^{-1} in 3 M H_2SO_4 electrolyte. The CNAG electrode exhibited a roughly capacitive signal over 900 mV range and there is no current peak caused by a

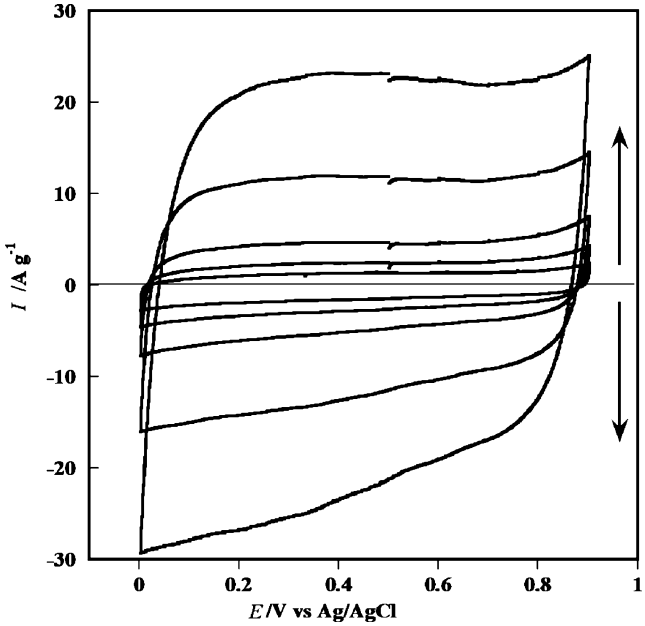

Fig. 1 Cyclic voltammograms of CNAG electrode recorded in 3 M H_2SO_4, potential range 0–0.9 V versus Ag/AgCl. Potential scan rates ranging from 5 to 100 mV s^{-1}. *Arrows* indicate direction ascending potential scan rate

redox reaction, indicating a typical electric double layer behavior. One can further note that the current increases with the increase of the scan rate with no significant degeneration of the shape of the CVs at the high scan rates.

Figure 2 compares galvanostatic charge–discharge curves at three electrodes CAG, CAG-3%MWNT, and CNAG. The curves are fairly linear for all the electrodes. It can be seen that a significant *iR* drop of 300 mV is displayed by the pristine CAG, whereas addition of MWNTs to the CAG decreased the *iR* drop to 150 mV, and to 30 mV with the CNAG electrode.

Specific capacitances determined from CC experiments as function of the applied current are reported in Fig. 3. First, it is clear that CNAG electrode displayed a more stable behavior with the applied current when compared to others. From the values of Fig. 3, the CNAG electrode delivered a mean specific capacitance of 280 F g^{-1} versus 232 F g^{-1} and 187 F g^{-1} for the CAG-3%MWNT and pristine CAG, respectively.

Figure 4 shows the cycle life of the CNAG electrode as compared to that of CAG and CAG-3%MWNT electrodes. The tests were performed for 5,000 of galvanostatic charge–discharge cycles at a current load of 4 mA for the three samples. For both the CAG and the CAG-3%MWNT an enhancement of the capacitance during cycling was observed. The enhancement was more remarkable with CAG-3%MWNT sample where very high capacitance of 500 F g^{-} was reached. Dramatically, after this capacitance enhancement, a sudden drop to very low values was observed with the CAG and CAG-3%MWNT. On the other hand, the CNAG electrode displayed outstanding stability and no drop in the specific capacitance occurred over the 5,000 cycles. It even showed an increase in the capacitance during cycling from 294 F g^{-1} at the first cycle to 326 F g^{-1} at the 5,000th cycle.

Similar electrochemical studies were conducted in 5 M KOH electrolyte. Figure 5 shows cyclic voltammograms recorded at the CNAG electrodes with various potential scan rates. A double layer capacitive behavior is displayed over a range of 800 mV. Here too, the current increased as the potential scan rate increased.

Figure 6 compares CC curves at three electrodes CAG, CAG-3%MWNT, and CNAG. The curves are fairly linear for all the electrodes. Decreased *iR* within the composite system is evident from the CCs, i.e., 47 mV and 97 mV for the CAG-3%MWNT and CNAG, respectively versus 211 mV with pristine CAG.

The cycle life of the CNAG electrode as compared to that of CAG and CAG-3%MWNT electrodes is presented in Fig. 7. The tests were performed for 5,000 of

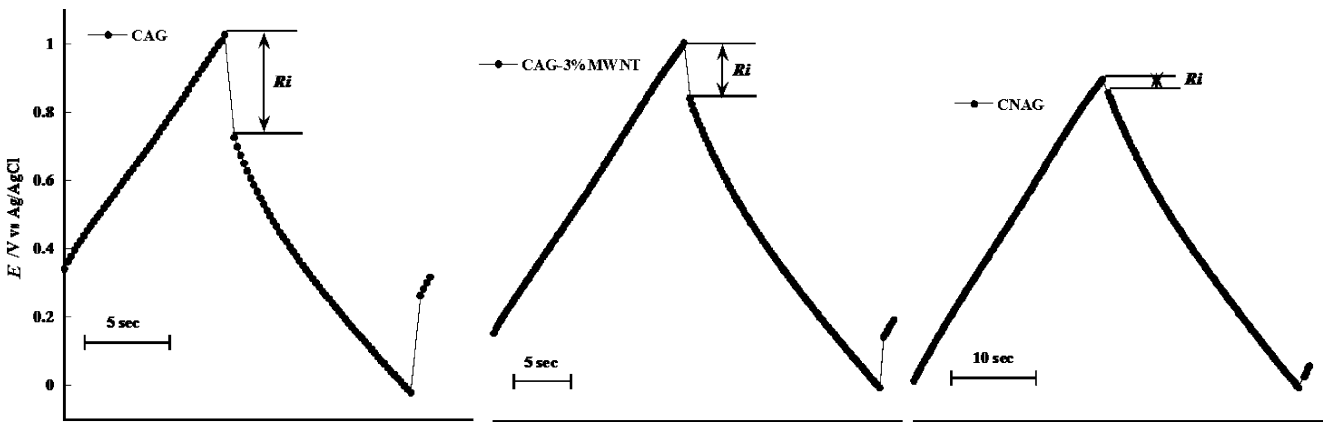

Fig. 2 Comparative galvanostatic charge–discharge curves of CAG, CAG-3%MWNT, and CNAG electrodes recorded in 3 M H_2SO_4, current loading of 4 mA

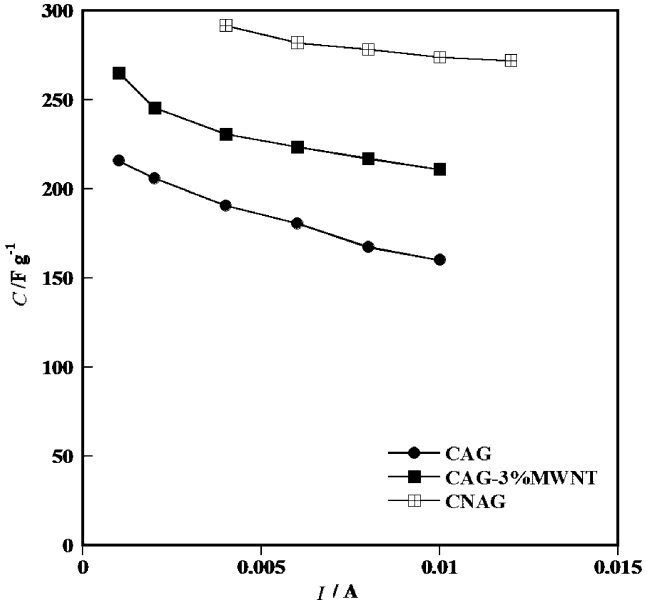

Fig. 3 Comparative variation of the specific capacitance as function of the current loading of CAG, CAG-3%MWNT, and CNAG electrodes during galvanostatic charge/discharge measurements in 3 M H_2SO_4

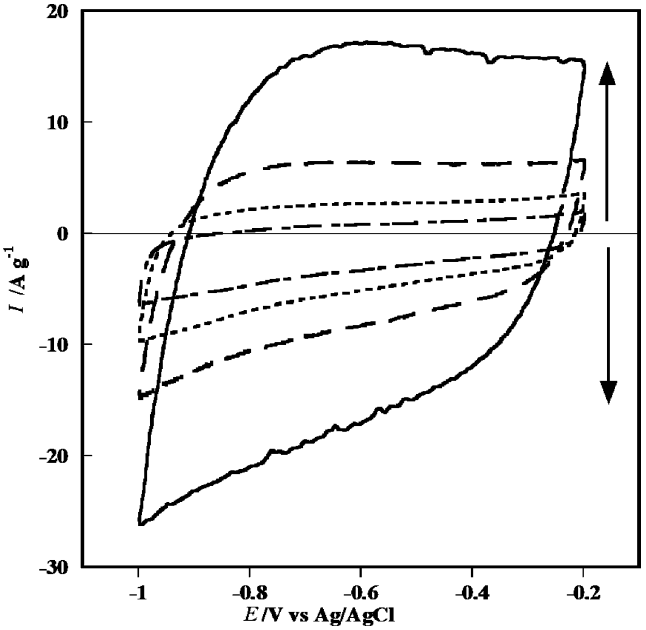

Fig. 5 Cyclic voltammograms of CNAG electrode recorded in 5 M KOH, potential range −0.2 to −1 V versus Ag/AgCl. Potential scan rates ranging from 5 to 100 mV s^{-1}. *Arrows* indicate direction ascending potential scan rate

galvanostatic charge–discharge cycles at a current load of 1 mA for the three samples. The CNAG electrode delivered an outstanding specific capacitance of 524 F g^{-1} at the first cycle. During the first hundred cycles, we observed a loss of 29% of the initial specific capacity for the CNAG as compared to 7.8% and 21% loss for the CAG and CAG-3% MWNT, respectively. Nevertheless, the CNAG maintained excellent stability after 500 cycles with a capacitance remaining as high as 400 F g^{-1}. For the time being, the capacitance fading during initial cycles is not understood but seems inherent in KOH electrolyte to all CAG composites either made by dispersion or by molding.

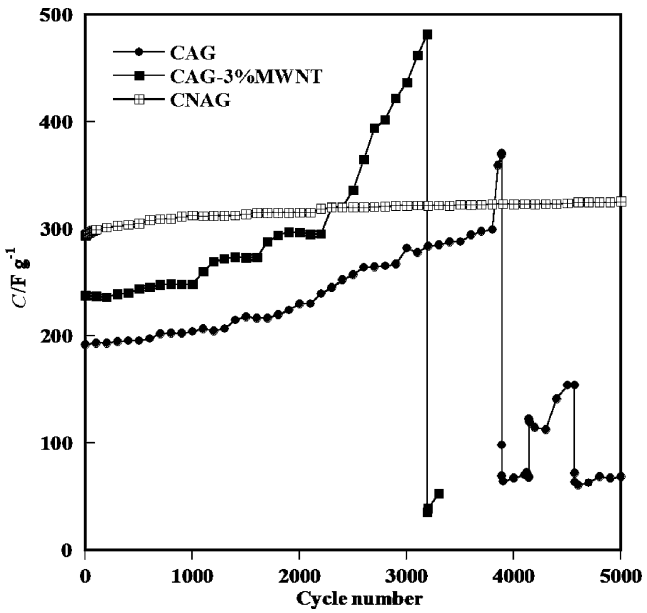

Fig. 4 Cycle life of CAG, CAG-3%MWNT, and CNAG composites electrodes upon 5,000 cycles in 3 M H_2SO_4

First, either in KOH or in H_2SO_4 electrolyte, the specific capacitance, C_s was found as follows: C_s(CNAG)> C_s(CAG-3%MWNT)>C_s(CAG). These results can be related to the SSA, CNAG (1,059 m^2 g^{-1})>CAG-3% MWNT (804 m^2 g^{-1})>CAG (660 m^2 g^{-1}); however, we have learned that for our composites, a higher SSA does not necessarily yield higher C_s [16]. It is rather the size and distribution of the pores that are likely among the key parameters that govern the capacitive performance of the CAG–CNT composites. The CAG and CAG–MWNTs prepared by dispersion process exhibited microporosity higher than 95% of the total SSA with all having dominant pore size diameter at around 0.57 nm. Nonetheless, an optimal performance is expected in the case of a porous nanostructured carbon of high specific surface area but also of well-balanced micromesoporosity. The micropore will participate in the charge storage processes and wide pathways, whereas the mesopore will permit fast accessibility to ions, thus a high energy at a high rate [19]. The micropores (ultramicropore) 0.7 nm and supermicropore (0.7–2 nm) play an essential role for ion adsorption, whereas the mesopores are necessary for their quick transportation to the bulk of material. If the pore volume is plotted versus the pore diameter (Fig. 8), it can be seen that all CAG–MWNT and CNAG composites displayed a

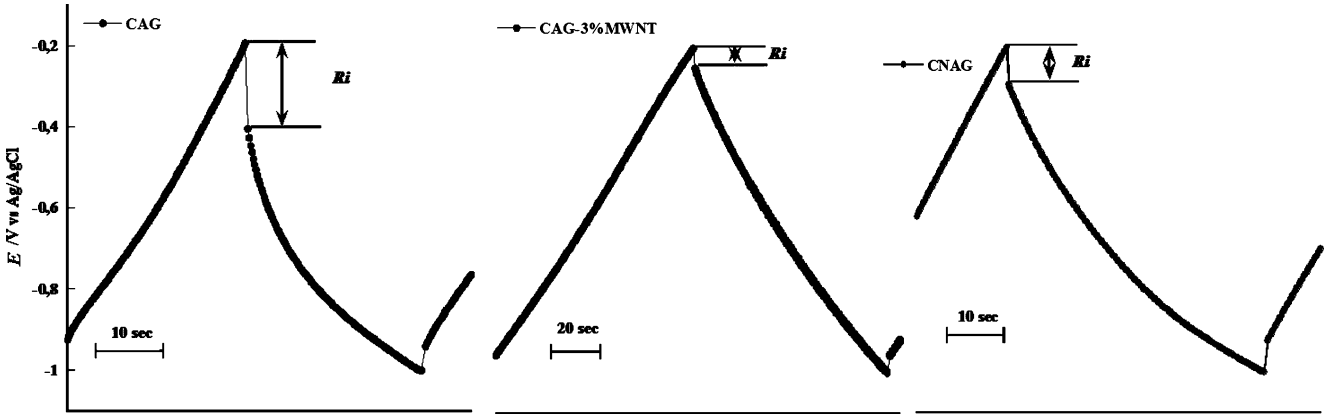

Fig. 6 Comparative galvanostatic charge–discharge curves at a current loading of 1 mA for CAG, CAG-3%MWNT, and CNAG electrodes recorded in 5 M KOH electrolyte

very different pore size distribution. The CAG-3%MWNT exhibited a narrow pore distribution with a dominant peak at 0.57 nm (ultramicropore <0.7 nm), whereas the CNAG showed two domains, a narrow domain peaking at 1.44 nm (supermicropore) and a wider domain within 2 to 10 nm (mesopore). A percentage of 50/50 (micropore/mesopore) constituted the total SSA of the CNAG samples. This well-balanced textural porosity explains very well the higher capacitive performance of the CNAG composite.

Besides the higher capacitive performance obtained with CNAG electrodes, the cycle life stability is another outstanding performance particularly in H_2SO_4 electrolyte. With CAG–MWNT synthesized by dispersion, we observed a remarkable increase in the capacitance which was followed by a dramatic drop to very low values similarly to the pristine CAG. We have ascribed the increase in C_s due to the ion intercalation bisulfate with cycling. Our interpretation is based on Kinoshita's work who reported that when graphite is anodically oxidized in a concentrated acid of the sulfuric acid, swelling (i.e., intercalation of bisulphate ions) and attack of the internal carbon atoms in the lattice plane occur [20]. Thus, due to continuous swelling, the pore network of the CAG and CAG-3% MWNTs composite totally collapses and induces a sudden fall in the capacitance. An interesting observation we made with CAG–MWNTs composite is that as much as the amount of MWNTs was increased, the drop in the capacitance was delayed and even disappeared after 12 wt.% of MWNTs; however, at the expense of the specific capacitance which was very much lower than the pristine CAG itself [16]. This was an indication that higher amounts of MWNTs provided a mechanical integrity to the

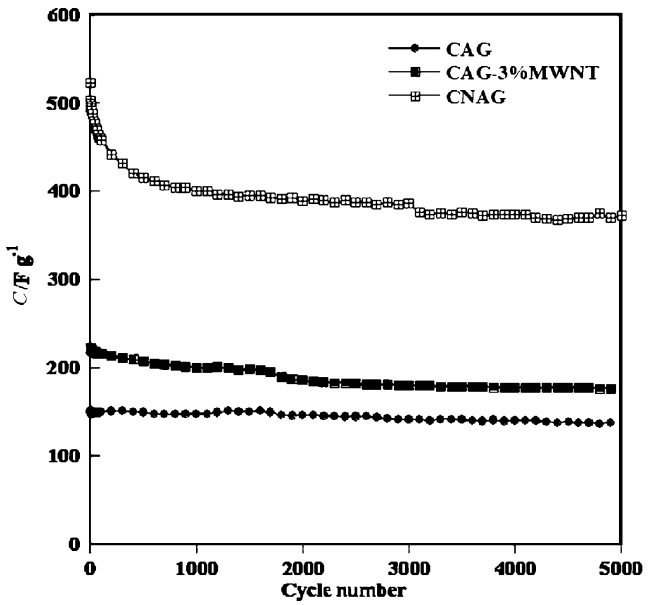

Fig. 7 Cycle life of CAG, CAG-3%MWNT and CNAG composites electrodes upon 5,000 cycles in 5 M KOH

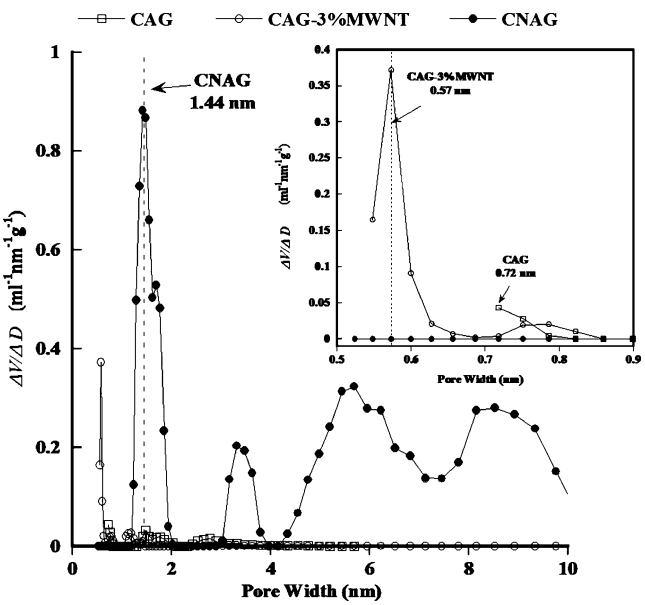

Fig. 8 Pore size distribution determined by density functional theory model for CAG and CAG–MWNT and CNAG composite electrodes

CAG's internal network because MWNTs have a high resistance to the electrochemical oxidation [21] and thus improved the resistance to the sulfuric acid attack, but in the meantime, it was obvious that dispersion of MWNTs within the CAG's pore network was not uniform but likely MWNTs agglomerated at some parts of the porous network since it yielded capacitance much lower than the CAG alone. Still a better way to uniformly disperse the MWNTs within the CAG network was needed to maintain the C_s of the CAG. The molding procedure clearly solved this issue and a capacitance much higher than the CAG alone accompanied by excellent cycle-life stability in H_2SO_4 electrolyte. This is due to an optimum reinforcement of the aerogel's network by the carbon nanotubes for the CNAG composites.

Conclusion

We have developed a new class of binderless carbon nanotubes aerogel (CNAG) composites that differ significantly from these previously reported in the literature. This composite material is synthesized by a CVD method to grow carbon nanotubes directly onto a microfibrous carbon paper substrate. Then the carbon aerogel is synthesized on the carbon nanotubes. The key feature of the method is eliminating the necessity of controlling the carbon nanotube concentration, which permits optimized dispersion processes to reinforce the aerogel's networks.

Because this new material combines a high specific surface area, a special textural porosity with the electrical conductivity of the carbon nanotubes it delivered very high specific capacitances of 524 F g^{-1} in KOH electrolyte and 280 F g^{-1} in H_2SO_4 electrolyte when used as an electrode in electrochemical double layer capacitors.

Furthermore, this better integration of carbon nanotubes in the matrix of carbon aerogel improved its resistance to the attack by the electrolyte and conferred an excellent cycle life over 5,000 cycles of charge–discharge.

The molding procedure for the preparation of nanocomposite by direct deposition of carbon aerogel onto carbon nanotubes represents an important step forward for improving the mechanical strength of the carbon aerogel. Owing to their unique physicochemical properties, the CNAG nanocomposites are also of great interest to a variety of energy conversion and storage applications, as material intercalation in lithium-ion batteries or as catalyst support in fuel cells, including biofuel cells.

Acknowledgments The authors would like to thank the Natural Sciences Engineering Research Council of Canada (NSERC), the Fonds Québécois pour la Recherche en Nature et Technologie (FQRNT), NanoQuébec, and the Centre Québécois pour les Matériaux Fonctionnels (CQMF).

References

1. Burke A (2000) J Power Sources 91:37
2. Aricò AS, Bruce P, Scrosati B, Tarascon J-M, Schalkwijk WV (2005) Nat Matters 5:366
3. Pekala RW, Farmer JC, Alviso CT, Tran TD, Mayer ST, Miller JM, Dunn B (1998) J Non-Cryst Solids 225:74
4. Gouérec P, Talbi H, Miousse D, Tran-Van F, Dao LH, Lee KH (2001) J Electrochem Soc 148:A94
5. Wei Y-Z, Fang B, Iwasa S, Kumagai M (2005) J Power Sources 141:386
6. Wang J, Zhang SQ, Guo YZ, Shen J, Attia SM, Zhou B, Zheng GZ, Gui YS (2001) J Electrochem Soc 148:D75
7. Talbi H, Just P-E, Dao LH (2003) J Appl Electrochem 33:465
8. Li W, Pröbstle H, Fricke J (2003) J Non-Cryst Solids 325:1
9. Long JW, Dening BM, McEvoy TM, Rolison DR (2004) J Non-Cryst Solids 350:97
10. Hwang SW, Hyun S-H (2004) J Non-Cryst Solids 347:238
11. Kim H-J, Kim J-H, Kim W-I, Suh DJ (2005) Korean J Chem Eng 22:740
12. Bordjiba T, Mohamedi M, Dao LH (2007) Nanotechnology 18:035202
13. Bordjiba T, Mohamedi M, Dao LH, Aïssa B, El Khakani MA (2007) Chem Phys Lett 441:88
14. Bordjiba T, Mohamedi M, Dao LH (2007) J Power Sources 172:991
15. Bordjiba T, Mohamedi M, Dao LH (2008) Electrochem Soc Trans 6:183
16. Bordjiba T, Mohamedi M, Dao LH (2008) J Electrochem Soc 155: A115
17. Bordjiba T, Mohamedi M, Dao LH (2008) Adv Mater 20:815
18. Aïssa B, Hamoudi Z, Takahashi H, Tohji K, Mohamedi M, El Khakani MA (2009) Electrochem Commun 11:862
19. Frackowiak E, Béguin F (2001) Carbon 39:937
20. Kinoshita K (1988) Carbon-electrochemical and physicochemical properties. Wiley, New York
21. Shao Y, Yin G, Zhang J, Gao Y (2006) Electrochim Acta 51:5853